

Enhancing the Versatility and Functionality of Fast Photochromic Bridged Imidazole Dimers by Flipping Imidazole Rings

Kentaro Shima,[†] Katsuya Mutoh,[†] Yoichi Kobayashi,[†] and Jiro Abe^{*,†,‡}

[†]Department of Chemistry, School of Science and Engineering, Aoyama Gakuin University, 5-10-1 Fuchinobe, Chuo-ku, Sagami-hara, Kanagawa 252-5258, Japan

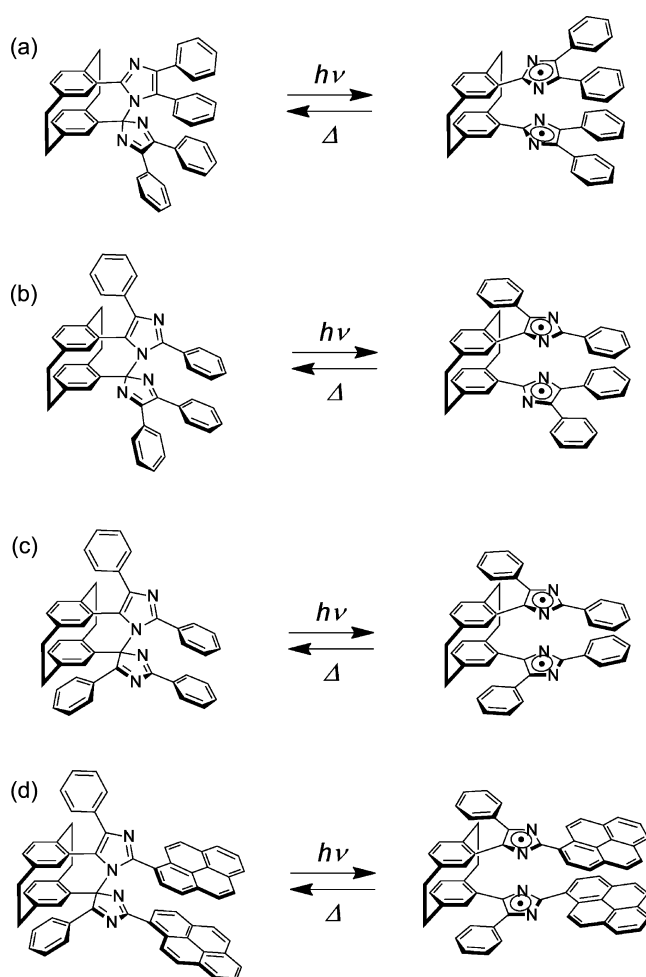
[‡]CREST, Japan Science and Technology Agency (JST), K's Gobancho, 7 Gobancho, Chiyoda-ku, Tokyo 102-0076, Japan

S Supporting Information

ABSTRACT: The widely tunable optical properties and the visible sensitivity have been required for fast photochromic molecules whose coloration–decoloration cycle completes in μs to ms time scale not only for practical applications such as full-color holographic displays but also for fundamental researches in biochemistry. However, the so far developed [2.2]paracyclophane-bridged imidazole dimers, which are one of the best candidates for fast photochromic molecules, have their weaknesses for these requirements. Herein, we overcome the issues with sustaining fast photochromism and high durability by flipping the two imidazole rings (the head-to-tail and tail-to-tail forms). The alteration in the relative configuration of the imidazole rings suppresses the broad absorption band resulting from the radical–radical interaction. The substitution to the 2-position of the imidazole ring of the tail-to-tail form gives the drastic changes in the steady-state and the transient absorption spectra. The pyrene-substituted tail-to-tail form demonstrates that the transient absorption spectrum is featured by the inherent spectrum of the imidazolyl radical. This molecular framework is easy to functionalize fast photochromic molecules such as sensitizations to the red light, chirality, and biological tagging, and therefore it is versatile for various fast photochromic applications.

The μs to ms time scale is one of the crucial time scales for human daily lives because signals within the time scale look instantaneous or cannot be detected by human eyes due to their time resolutions (within a few tens of ms) but can be easily detected by simple mechanical instruments. Photochromic molecules, which reversely react upon light irradiation,^{1,2} could act as excellent probes and triggers to reveal and control phenomena which occur under these time scales. However, there were few photochromic molecules whose coloration–decoloration cycle completes in the μs to ms time scale.^{3,4} *Pseudogem*-bisDPI[2.2]PC (HH in Scheme 1a), which is one of the best candidates for fast photochromic molecules, has a tunable photochromic reaction in the time range from μs to hundreds of ms with near unity quantum efficiency and excellent durability.^{5,6} *Pseudogem*-bisDPI[2.2]PC has opened up various potential applications in industry such as holographic displays^{7,8} and security-recognition devices.⁹ However, their applications were restricted to the modulation of the total

Scheme 1. Photochromism of (a) HH, (b) HT, (c) TT, and (d) Py-TT



absorbance or reflection of light with time because of the following two reasons: (1) the broad transient absorption band due to the radical–radical interaction restricted the color selectivity and (2) the effect of substitution was moderate and therefore the functionalization was restricted.^{10,11} The spectral tunability and the visible-light sensitivity would expand the

Received: February 4, 2014

Published: February 24, 2014

potentials of fast photochromic molecules into full-color holographic displays¹² eventually for commercially available televisions, wavelength-selective high security systems, and color-selective filters for detectors to avoid instantaneous saturations of light. In addition to industrial applications, fast photochromic molecules which respond to visible light can be used as a trigger pulse to induce unfolding of proteins,^{13,14} motions of protein motors,¹⁵ and isomerization of DNAs,^{16,17} and they offer a possibility to observe dynamic conformation changes in real time.

In this study, we overcome these issues with sustaining fast photochromism and high durability by flipping both imidazole rings of *pseudogem*-bisDPI[2.2]PC. The alteration in the relative configuration of the imidazole rings suppresses the broad absorption band due to the radical–radical interaction. When we call *pseudogem*-bisDPI[2.2]PC as the head-to-head form (**HH**), in which the 2-position of both imidazole rings binds to a [2.2]paracyclophane (PC) moiety, we synthesized the head-to-tail form of *pseudogem*-bisDPI[2.2]PC (**HT**, Scheme 1b) and the tail-to-tail form of *pseudogem*-bisDPI[2.2]PC (**TT**, Scheme 1c), in which the 4-position of one of the imidazole ring or both imidazole rings bind to the [2.2]PC moiety. The 2-position of the imidazole ring of the tail-to-tail form is easily substituted by using aldehyde derivatives, and the substituent can drastically modulate both steady-state and transient absorption spectra. The aldehyde derivatives are widely available in various companies and are much easier to synthesize as compared to diketone derivatives, which are necessary to substitute the head-to-head form. As a demonstration, we attached two pyrenes to the 2-position of both imidazole rings of the tail-to-tail form of the bridged imidazole dimer (**Py-TT**, Scheme 1d) and showed how the spectra drastically changes. Fast photochromic molecules with the wavelength tunability and the visible sensitivity have potentials to develop novel practical applications and to establish new academic fields.

Scheme 1 illustrates the photochromism of **HH**, **HT**, **TT**, and **Py-TT**, respectively. The process of their photochromism is identical irrespective of the configuration of the imidazole rings. Upon UV irradiation, the radical pair, which is the origin of the coloration, is generated by the C–N bond cleavage, and two radicals thermally recombine and recreate the C–N bond. The steady-state absorption spectra of **HT** and **TT** slightly shift to the red region as compared to that of **HH**, which gradually increases from ~ 370 nm (Figures S21 and S22), but their spectral shapes are generally similar. Figure 1 shows transient absorption spectra of **HH**, **HT**, and **TT**. The vertical lines indicate the theoretical spectra for the colored species obtained by the TDDFT calculations (UMPW1PW91/6-31+G(d,p)//UM052X/6-31G(d)). The insets show ORTEP representations of their molecular structures obtained by X-ray crystallographic analysis. As we see from the structures, while the C–N bonds of **HH** and **HT** bind the 1- and 2'-position of the imidazole rings (1,2'-isomers), **TT** is the 1,4'-isomer. **HT** is intrinsically different from the head-to-tail form of the naphthalene-bridged imidazole dimer, which is the 1,4'-isomer.¹⁸ As shown in Figure 1a, we observe a strong absorption band around 400 nm and a broad absorption band over the visible region for **HH**. The TDDFT calculations indicate that two bands at ~ 400 and 500–600 nm are attributed to the imidazolyl radical, and the band over 600 nm is attributed to the radical–radical interactions, which are supported by our previous report.¹⁹ The transient absorption spectrum of **HT** shows the similar spectrum to that

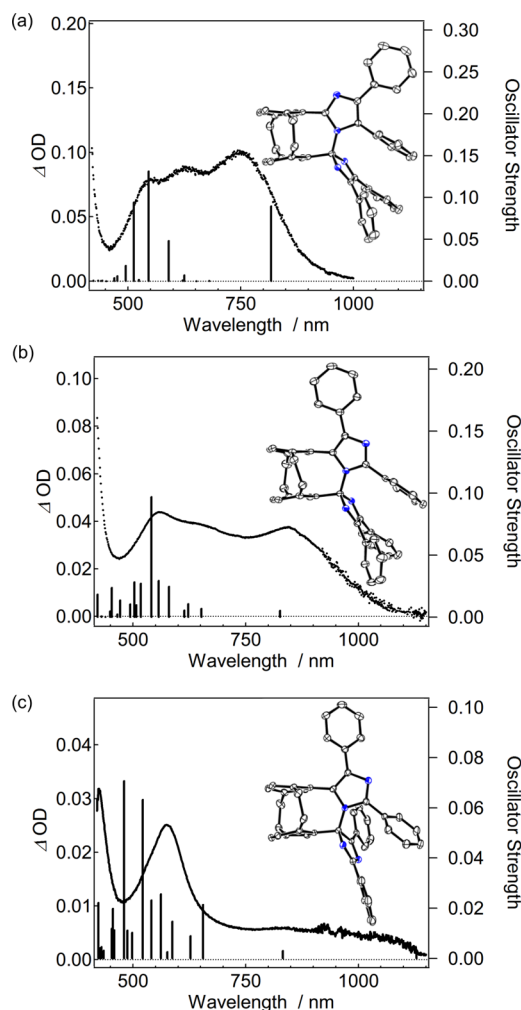


Figure 1. Transient absorption spectra of (a) **HH**, (b) **HT**, and (c) **TT** in degassed benzene (excitation wavelength, 355 nm; pulse width, 5 ns; power 4 mJ/pulse; the concentrations of **HH**, **HT** and **TT** are 2.1×10^{-4} , 2.2×10^{-4} and 1.1×10^{-4} M, respectively). Vertical lines indicate the theoretical spectra for the colored species of each molecule (TDDFT UMPW1PW91/6-31+G(d,p)//UM052X/6-31G(d)). Insets show ORTEP representations of the molecular structures obtained by X-ray crystallographic analysis.

of **HH**, but the absorption band derived from the radical–radical interaction decreases and shifts to the red region (Figure 1b). The decrease and the shift are more pronounced in the transient absorption spectrum of **TT**, while the absorption band due to the imidazolyl radical is similar to each other (Figure 1c). The transient absorption spectrum of **TT** has little absorption around the red region, and only the absorption band due to the imidazolyl radical is observed because of the reduced overlap integral of the wave function. The decrease in the radical–radical interaction is caused by the increase in the distance and the displacement between two imidazole rings. The optimized geometries of the colored species of **HH**, **HT**, and **TT** are shown in Figures S39, S43, and S47, respectively. The absorption band derived from the radical–radical interaction is red-shifted in the order corresponding to **HH**, **HT**, and **TT**. These absorption bands are mainly attributed to the HOMO–LUMO transition from the orbital localized at an imidazole ring to the orbital localized at the other imidazole ring.

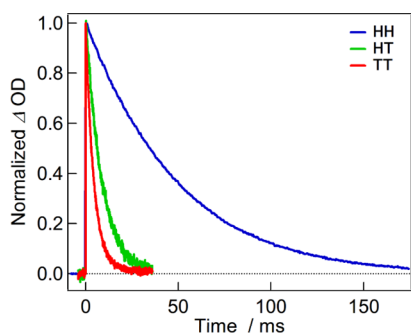


Figure 2. Decay profiles of the colored species generated from **HH**, **HT**, and **TT** at 298 K. Experimental condition is identical to that described in Figure 1.

Figure 2 shows the decay profiles of the colored species generated from **HH**, **HT**, and **TT** observed at 400 nm at 298 K. We also conducted the same experiments in aerated solutions and confirmed that the oxygen did not influence the spectra and the decay profiles. It indicates that **HH**, **HT**, and **TT** do not form any oxygen adducts as was found in the naphthalene-bridged imidazole dimer.²⁰ All decays are well fitted with a single exponential decay function, and the decay of the colored forms of **TT** and **HT** is faster than that of **HH** (Table 1). The half-lives ($\tau_{1/2}$) of the colored species of **HH**, **HT**, and **TT** are 33, 6.9, and 3.2 ms at 298 K, respectively. It is intuitively interpreted that the faster decay is caused by the destabilization of the colored species due to the repulsion between a phenyl group of the tail-aligned imidazole ring and the [2.2]PC moiety. The activation parameters (ΔH^\ddagger , ΔS^\ddagger , and ΔG^\ddagger at 298 K) were obtained from the analysis of the temperature dependence of the decay curves (Table 1). We found that all activation parameters decreased in the order corresponding to **HH**, **HT**, and **TT**. These results are consistent with those obtained from the theoretical calculations.

As a demonstration to show how the tail-to-tail form effectively modulates its spectrum, we synthesized **Py-TT**, in which the 2-position of two imidazole rings is substituted with two pyrenes. Figure 3a shows the absorption spectra of **TT**, the hexaarylbiimidazole derivative whose phenyl group at the 2-position of the imidazole ring is substituted with a pyrenyl group (**Py-HABI**) and **Py-TT**. As compared to the previous report of the head-to-head form derivatives whose 4-position of the imidazole ring is substituted with the pyrenyl group (**Py-HH**),¹¹ whose absorption spectrum shifts at most tens of nm, that of **Py-TT** largely shifts ~ 100 nm to the red. We found that **Py-TT** can be excited even at the wavelength longer than 500 nm (the threshold is ~ 550 nm, Figures S34–S36). The further sensitization to the red, which is the best region for biological probes,¹⁷ is easily accomplished by substituting the longer π -conjugated units. It demonstrates that the substitution to the 2-position of the imidazole ring of the tail-to-tail form is an

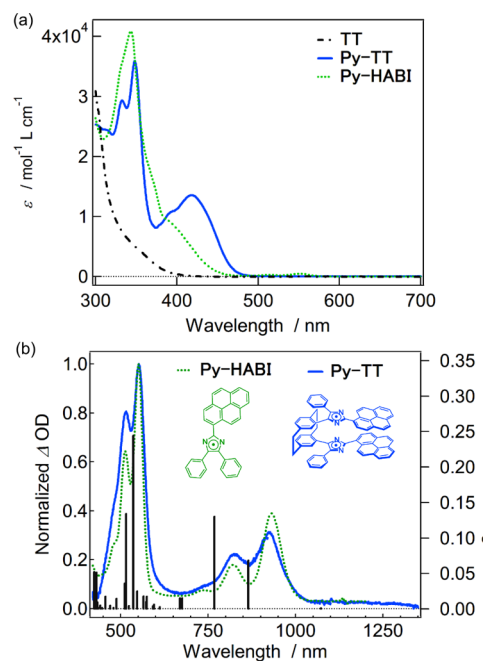


Figure 3. (a) Steady-state absorption spectra of **TT**, **Py-TT**, and **Py-HABI** in degassed benzene and (b) the transient absorption spectra of **Py-TT** and **Py-HABI**. Vertical lines indicate the theoretical spectrum for the colored species of **Py-TT** (TDDFT UMPW1PW91/6-31+G(d,p)//UM052X/6-31G(d)).

efficient tool to sensitize the visible light. The transient absorption spectrum of **Py-TT** is completely different from that of **Py-HH**. Interestingly, the transient absorption spectrum of **Py-TT** is almost identical to that of **Py-HABI** (Figure 3b).²¹ It shows that the substitution to the 2-position of the tail-to-tail form drastically modulates the transient absorption spectrum, and the spectrum is defined only by the imidazolyl radical, i.e., the radical–radical interaction is no longer observed. The imidazolyl radical gives the narrower transient absorption spectrum than the spectrum due to the radical–radical interactions, and it is easier to estimate by quantum chemical calculations. **Py-TT** is the first bridged imidazole dimer which exhibits a red coloration upon UV irradiation. Since the tail-to-tail form allows us to tune the transient colors simply by changing the substituents from the phenyl to pyrenyl groups with the similar decoloration time, the tail-to-tail form offers a great opportunity to develop a real-time RGB full-color holographic display, which has not been developed until now because of the lack of these kinds of materials. The half-life of the colored species of **Py-TT** is 1.4 ms at 298 K, and the activation parameters are shown in the Table 1. Moreover, the absorbance of the colored species of **Py-TT** decreases only several percent even after 10 000 shots of the 355 nm laser pulses (the pulse duration and the power is 5 ns and 4 mJ,

Table 1. Decoloration Reaction Rates, Half-Lives at 298 K, and Activation Parameters of the Colored Species of **HH**, **HT**, **TT** and **Py-TT** in Degassed Benzene^a

	k [s^{-1}]	$\tau_{1/2}$ [ms]	ΔH^\ddagger [kJ/mol]	ΔS^\ddagger [J/mol·K]	ΔG^\ddagger [kJ/mol]
HH	21	33	58.8 (70.3)	−22.2 (−10.5)	65.5 (72.6)
HT	1.0×10^2	6.9	52.8 (57.8)	−29.2 (−32.4)	61.5 (60.0)
TT	2.2×10^2	3.2	48.2 (50.5)	−38.1 (−62.8)	59.6 (54.9)
Py-TT	4.8×10^2	1.4	46.5	−37.8	57.7

^aValues in parentheses show calculated ones.

respectively, Figure S37), indicating a high fatigue resistance of Py-TT.

In conclusion, we designed the head-to-tail and tail-to-tail forms of the bridged imidazole dimer and systematically analyzed the effect of the relative configuration of the imidazole rings on the photochromic properties. Py-TT achieved visible sensitizations, and no radical–radical interactions were confirmed in the absorption spectrum of the colored species, which offers the tunable transient color selectivity from blue to red. This molecular framework is easy to functionalize fast photochromic molecules such as sensitizations to the red light, chirality, and biological tagging, and therefore it is versatile for various fast photochromic applications.

■ ASSOCIATED CONTENT

📄 Supporting Information

Experimental details and characterization data. This material is available free of charge via the Internet at <http://pubs.acs.org>.

■ AUTHOR INFORMATION

Corresponding Author

jiro_abe@chem.aoyama.ac.jp

Notes

The authors declare no competing financial interest.

■ ACKNOWLEDGMENTS

This work was supported partly by the Core Research for Evolutional Science and Technology (CREST) program of the Japan Science and Technology Agency (JST) and a Grant-in-Aid for Scientific Research (A) (22245025) from Ministry of Education, Culture, Sports, Science and Technology (MEXT), Japan. K. M. appreciates the Research Fellowships of JSPS for Young Scientists.

■ REFERENCES

- (1) Delaire, J. A.; Nakatani, K. *Chem. Rev.* **2000**, *100*, 1817.
- (2) Irie, M. *Chem. Rev.* **2000**, *100*, 1685.
- (3) Tomasulo, M.; Sortino, S.; Raymo, F. M. *Org. Lett.* **2005**, *7*, 1109.
- (4) Sousa, C. M.; Pina, J.; de Melo, J. S.; Berthet, J.; Delbaere, S.; Coelho, P. J. *Org. Lett.* **2011**, *13*, 4040.
- (5) Kishimoto, Y.; Abe, J. *J. Am. Chem. Soc.* **2009**, *131*, 4227.
- (6) Harada, Y.; Hatano, S.; Kimoto, A.; Abe, J. *J. Phys. Chem. Lett.* **2010**, *1*, 1112.
- (7) Ishii, N.; Kato, T.; Abe, J. *Sci. Rep.* **2012**, *2*, 819.
- (8) Ishii, N.; Abe, J. *Appl. Phys. Lett.* **2013**, *102*, 163301.
- (9) Iftime, G.; Breton, M. P.; Lee, F. P.-H.; Valeriu, A. M.; Chopra, N.; Odell, P. G.; Moorlag, C. Photochromic security enabled ink for digital offset printing applications. U.S. Patent 20130305947 A1, 2012.
- (10) Mutoh, K.; Abe, J. *J. Phys. Chem. A* **2011**, *115*, 4650.
- (11) Yamashita, H.; Abe, J. *J. Phys. Chem. A* **2011**, *115*, 13332.
- (12) Senoh, T.; Mishina, T.; Yamamoto, K.; Oi, R.; Kurita, T. *J. Disp. Technol.* **2011**, *7*, 382.
- (13) Muramatsu, S.; Kinbara, K.; Taguchi, H.; Ishii, N.; Aida, T. *J. Am. Chem. Soc.* **2006**, *128*, 3764.
- (14) Lindorff-Larsen, K.; Piana, S.; Dror, R. O.; Shaw, D. E. *Science* **2011**, *334*, 517.
- (15) Hoersch, D.; Roh, S.-H.; Chiu, W.; Kortemme, T. *Nat. Nanotechnol.* **2013**, *8*, 928.
- (16) Blanco-Lomas, M.; Samanta, S.; Campos, P. J.; Woolley, G. A.; Sampedro, D. *J. Am. Chem. Soc.* **2012**, *134*, 6960.
- (17) Samanta, S.; Beharry, A. A.; Sadowski, O.; McCormick, T. M.; Babalhavaej, A.; Tropepe, V.; Woolley, G. A. *J. Am. Chem. Soc.* **2013**, *135*, 9777.
- (18) Mutoh, K.; Shima, K.; Yamaguchi, T.; Kobayashi, M.; Abe, J. *Org. Lett.* **2013**, *15*, 2938.
- (19) Mutoh, K.; Nakano, E.; Abe, J. *J. Phys. Chem. A* **2012**, *116*, 6792.
- (20) Hatano, S.; Abe, J. *Phys. Chem. Chem. Phys.* **2012**, *14*, 5855.
- (21) Miyasaka, H.; Satoh, Y.; Ishibashi, Y.; Ito, S.; Nagasawa, Y.; Taniguchi, S.; Chosrowjan, H.; Mataga, N.; Kato, D.; Kikuchi, A.; Abe, J. *J. Am. Chem. Soc.* **2009**, *131*, 7256.